ELSEVIER

Journal of Nuclear Materials 249 (1997) 91–102

journal of nuclear materials

# Mechanisms for decoration of dislocations by small dislocation loops under cascade damage conditions

H. Trinkaus [a,*], B.N. Singh [b], A.J.E. Foreman [c]

[a] *Institut für Festkörperforschung, Forschungszentrum Jülich, D-52425 Jülich, Germany*
[b] *Materials Research Department, Risø National Laboratory, DK-4000 Roskilde, Denmark*
[c] *Materials Performance Department, Harwell Laboratory, Oxfordshire OX11 0RA, England, UK*

Received 25 March 1997; accepted 7 July 1997

**Abstract**

In metals under cascade damage conditions, dislocations are frequently found to be decorated with a high density of small clusters of self-interstitial atoms (SIAs) in the form of dislocation loops, particularly during the early stages of the microstructural evolution in well annealed pure metals. This effect may arise as a result of either (a) migration and enhanced agglomeration of single SIAs in the form of loops in the strain field of the dislocation or (b) glide and trapping of SIA loops (produced directly in the cascades) in the strain field of the dislocation. In the present paper, both of these possibilities are examined. It is shown that the strain field of the dislocation causes a SIA depletion in the compressive as well as in the dilatational region resulting in a reduced rather than enhanced agglomeration of SIAs. (SIA depletion may, however, induce enhanced vacancy agglomeration near dislocations.) The decoration of dislocations by SIA loops is therefore considered to be due to the trapping of glissile loops. Conditions for the operation of this mechanism are discussed. © 1997 Elsevier Science B.V.

## 1. Introduction

Generally, defect accumulation in crystalline solids under irradiation has been considered to occur in an essentially homogeneous mode. Accordingly, this process has been modeled within the framework of a mean field chemical rate theory approach [1,2] in which the following assumptions are made: (1) both vacancies and self-interstitial atoms (SIAs) are produced as monodefects, randomly in space and time, (2) clusters of both types of defects result from the three-dimensional diffusion and reaction of these monodefects, and (3) these clusters are immobile.

It has been found, however, that the evolution of void and dislocation microstructures under cascade damage conditions (particularly in well annealed pure metals at low dose irradiations in the temperature range of annealing stage IV) occurs in a non-homogeneous and segregated fashion: The two most striking features, first observed already more than a quarter of a century ago, are: (1) the enhanced swelling in several μm wide regions adjacent to grain and subgrain boundaries [3–5] (for further references, see Refs. [6–8]), and (2) the formation of patches or 'rafts' of dislocation loops [3,9–15] and the decoration of grown-in dislocations (with an edge component) by loops [3,15–20] which may even extend to form dislocation walls [20–23]. The latter features are the subject of the present paper (for experimental details, see Section 2).

Decoration of dislocations with loops plays a key role in the discussion of radiation hardening under cascade damage conditions presented in an accompanying paper [24]. It is shown there that characteristic features in the deformation behaviour of metals and alloys under cascade damage conditions such as the increase of the upper yield stress without dislocation generation followed by a yield

* Corresponding author. Tel.: +49-2461 616 460; fax: +49-2461 612 620.


*PII* S0022-3115(97)00230-4

drop and plastic instability cannot be rationalized in terms of the conventional radiation hardening model commonly known as 'dispersed barrier hardening' (DBH) model in which a distribution of (rigid) obstacles in the form of precipitates or defect clusters is assumed to act against the dislocation motion. As an alternative, a 'cascade induced source hardening' (CISH) model is proposed in which a dislocation decorated with loops, like a Cottrell atmosphere of impurities [25], is assumed to be locked so firmly that it cannot act as a dislocation source until the applied stress reaches a very high level [24].

Principally, there are two main mechanisms which could result in the decoration of a dislocation with loops: (1) The sweeping of glissile SIA loops during the motion of the dislocation [26], and (2) the accumulation of SIAs near the dislocation by SIA transport. In most of the cases quoted above, the operation of the first mechanism can be ruled out on the basis of the fact that the accumulation process continues even when the dislocations are obviously locked. For SIA transport to and accumulation near a dislocation it is useful to distinguish two possibilities: (a) the three-dimensional migration and possibly enhanced agglomeration of single SIAs in the form of loops in the strain field of the dislocation, or (b) the glide and trapping of small SIA loops, directly produced in cascades, in the strain field of the dislocation.

In the present paper, it is first shown (in Section 3) that decoration of a dislocation by loops cannot be rationalized in terms of strain enhanced agglomeration of single three-dimensionally migrating SIAs. In this discussion, the possibility of enhanced vacancy agglomeration close to dislocations is included. Then (in Section 4), the second possibility is considered as a realistic alternative. In fact, already Brimhall and Mastel [9] have discussed the formation of loops rafts and dislocation decoration by loops in terms of loop glide combined with self-climb. In their discussion, however, the origin of the small primary SIA loops and the driving force for their long range migration remained unclear.

To understand the role of displacement cascades in the decoration process it is important to recognize the specific features of cascades. It is now well established by experimental (for reviews see Refs. [6,7]) and molecular dynamics (MD) studies [27–30] that in displacement cascades vacancies and SIAs are generated in a highly localized and segregated fashion resulting in efficient clustering of both types of defects. Small SIA loops have been found in MD studies to be highly glissile [29]. Such a loop is expected to perform a thermally activated random glide motion by which it may leave its native cascade region and migrate over large distances until it gets trapped directly by or in the strain field of another defect such as a dislocation. We conclude this introduction by reminding the reader of an asymmetry in the behaviour of interstitial and vacancy clusters [7]: in contrast to small SIA loops, small vacancy loops are not known to be glissile.

## 2. Experimental evidence

Even though the decoration of dislocations by clusters of SIAs in the form of small loops is a striking effect this phenomenon has not been investigated systematically in the past. As a result, the available evidence on dislocation decoration is rather limited and scattered. Nevertheless, the existing amount of experimental evidence, at least in pure metals and simple alloys, is enough to justify investigations of possible mechanisms capable of causing an extensive atmosphere of SIA loops around a grown-in dislocation line. It should be added that since the grown-in dislocations act as sinks for vacancies and SIAs, the phenomenon of dislocations decoration is rather intriguing and does deserve an explanation.

Let us first consider the case of electron irradiation where defects are produced in the form of isolated Frenkel pairs. In this case, accumulation of vacancies in the form of stacking fault tetrahedra within the compressional field of edge dislocation have been observed occasionally [31–33]. An example of electron-irradiated Ag is shown in Fig. 1 [32].

In the present context, a comparison of electron irradiation and cascade damage effects in one material (or two similar materials) at similar temperatures is of particular interest. Fig. 2a shows an example of Ni–0.3 at.% Ge irradiated with 1 MeV electron at 473 K [19]. It can be easily seen that there is no sign of any accumulation of loops at or in the vicinity of the grown-in dislocations. In the case of neutron irradiated Ni–0.2 at.% Ge, on the other hand, a large number of dislocation loops are formed at or/and in the vicinity of a grown-in dislocation (Fig. 2b) [19]. Thus, this decoration phenomenon seems to require cascade damage conditions.

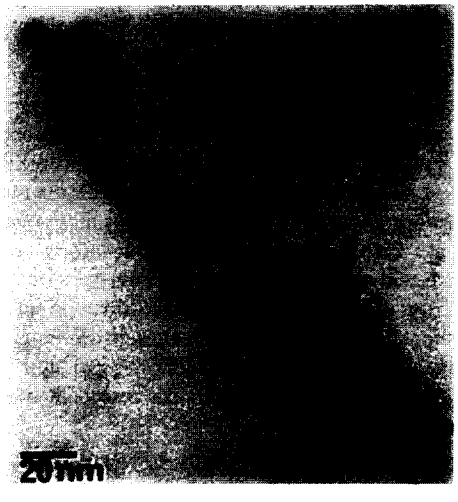


Fig. 1. An example of a dislocation line decorated with vacancy SFT, in silver irradiated with 1 MeV electrons at 330 K in a high voltage electron microscope [32].

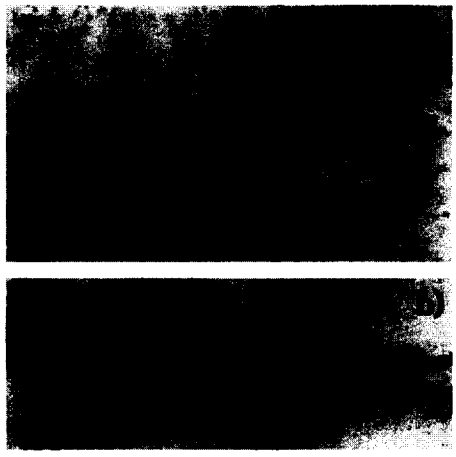

Fig. 2. (a) An electron micrograph showing an absence of dislocation decoration in a thin foil of Ni–0.3 at.% Ge irradiated with 1 MeV electrons at 473 K to a fluence level of $3.6\times10^{25}$ e/m$^2$ (0.2 dpa) [19]. (b) A dislocation line heavily decorated with interstitial loops in Ni–2 at.% Ge (bulk) irradiated with 14 MeV neutrons at 563 K to a fluence level of $6\times10^{22}$ n/m$^2$ ($2\times10^{-2}$ dpa) [19].

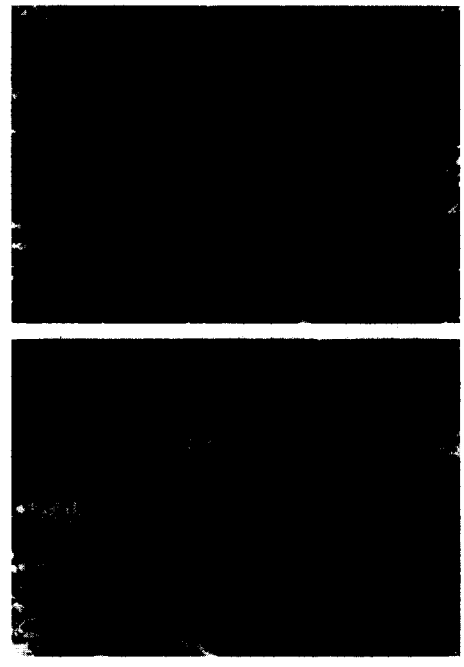

Fig. 3. Dislocations decorated with loops/clusters in pure nickel irradiated (in bulk) with 14 MeV neutrons at (a) 300 K ($6\times10^{21}$ n/m$^2$) and (b) 560 K ($6.2\times10^{22}$ n/m$^2$) [16].

While the accumulation of vacancy clusters near dislocations under electron irradiation is a rather rare case, decoration of dislocations by small interstitial loops under cascade damage conditions seems to be a common phenomenon. The latter has been observed, for instance, in pure nickel irradiated with 14 MeV neutrons at 300 K [16], and 563 K [17]. Kojima et al. [17] made similar observations in Ni–2 at.% Cu and Ni–2 at.% Ge alloys irradiated at 563 K with 14 MeV neutrons. However, no such decorations where observed in Ni–Si and Ni–Sn alloys. Examples of dislocation decoration by small interstitial loops in pure nickel irradiated with neutrons at 300 and 560 K are shown in Fig. 3 [16].

The accumulation of interstitial loops at and near grown-in dislocations has been also reported for pure copper and copper alloys irradiated with 14 MeV neutrons at 473 K [18]. The grown-in dislocation segments have been observed to be decorated by small loops in OPFHC-copper (99.999% pure) irradiated at 320 K with fission neutrons [20]. In pure copper irradiated at 523 K, interstitial loops segregate at grown-in dislocations to the extent that dislocation 'walls' are created [20–23]; an example of such a wall is shown in Fig. 4 [20].

Recently dislocation decoration has been observed in a pure single crystal of molybdenum (Fig. 5a) irradiated with fission neutrons at 320 K [15]. Fig. 5 also shows examples of rafts of dislocation loops formed in molybdenum single crystals irradiated at 320 K (Fig. 5b) [15] and polycrystalline Mo irradiated at 773 K (Fig. 5c) [13]. In fact, the first observation of raft formation in Mo and TZM (Mo, 0.5%, Ti, 0.1 Zr) have been reported by Brimhall and Mastel already in 1970 [9]. Since then a number of subsequent observation of raft formation in Mo and TZM have been reported [10–15]. The general consensus is that the rafts are clusters of small interstitial loops, all having the

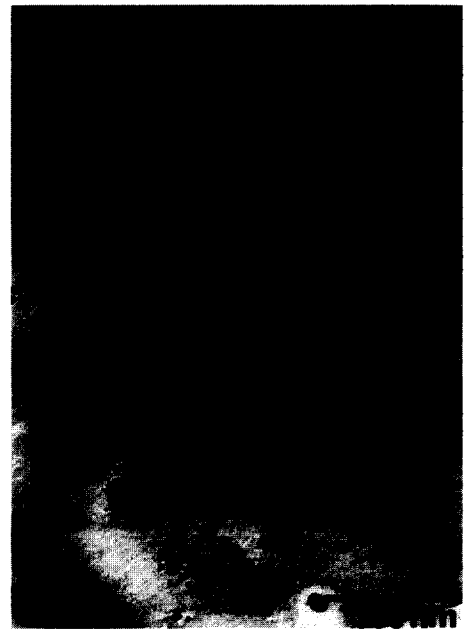

Fig. 4. An example of dislocation wall formation in pure copper irradiated with fission neutrons at 523 K [20] to a fluence level of $5\times10^{22}$ n/m$^2$ ($10^{-2}$ dpa, $E>1$ MeV).

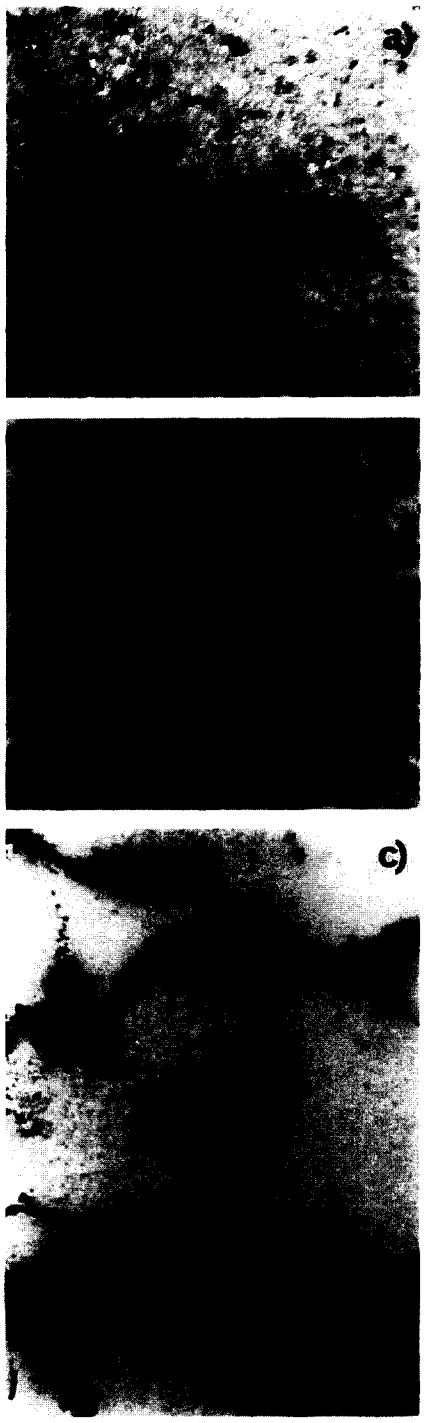


Fig. 5. Examples of dislocation decoration and 'raft' formation in molybdenum irradiated with fission neutrons: (a) dislocation decoration in a single crystal Mo irradiated at 320 K to a fluence of $5\times10^{21}$ n/m$^2$ ($E>1$ MeV) [15], (b) 'rafts' in a single crystal Mo irradiated at 320 K to a fluence of $1.5\times10^{24}$ n/m$^2$ ($E>1$ MeV) [15], and (c) 'rafts' in polycrystalline Mo irradiated at 773 K to a fluence of $8.1\times10^{24}$ n/m$^2$ ($E>1$ MeV) [13].

same Burgers vector, the rafts as a whole having a clear (111) habit plane identical to the Burgers vector of the loops.

Raft formation, dislocation decoration and dislocation wall formation appear to be related loop accumulation phenomena. In the following we focus on the decoration of dislocations with loops.

## 3. Clustering of single SIAs and vacancies near dislocations

In discussing the phenomenon of irradiation induced decoration of dislocations with small SIA clusters in the form of dislocation loops, it is frequently argued that the nucleation and growth of such clusters would be favoured in the region of positive dilatational strain in the neighbourhood of a dislocation where the elastic interaction between the dislocation and the SIAs is attractive [16]. This possibility will be examined in the following section including its counterpart, i.e., the possibility of enhanced vacancy agglomeration.

The (biased) accumulation and absorption of radiation induced defects at or by dislocations is controlled by the

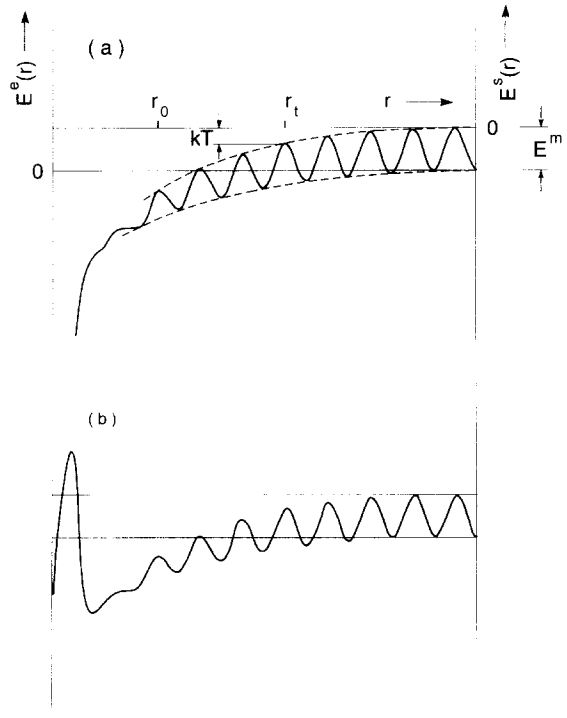


Fig. 6. One-dimensional sketch of two characteristic potential energy profiles for a point defect (self-interstitial) near a dislocation. In cases a and b, the defect annihilation is taken to be diffusion and reaction limited, respectively. $E^m$ is the migration energy in undistorted regions and $E^s(r)$ and $E^e(r)$ are interaction energies in metastable equilibrium and saddle point sites, respectively, with $E^s(r_t) = -kT$ where $r_t$ is the trapping radius.

interaction between the two components. In Fig. 6, two characteristic types of attractive interaction energy profiles felt by a defect (SIA or vacancy) near a dislocation are sketched. The most likely first case illustrated in Fig. 6a is characterized by a continuous decrease of both the stress/strain induced changes of the metastable equilibrium energy $E^e(r)$ and the saddle point energy $E^s(r)$ with decreasing distance, $r$, from the dislocation, even up to the dislocation core. The effective trapping radius $r_t$ is defined by the position where $E^s(r)$ falls short of the thermal energy $kT$; no metastable equilibrium position exists below the stability limit $r_o$. In this case, the dislocation would act as a perfect sink for SIA annihilation which would therefore be diffusion limited. The less likely second case illustrated in Fig. 6b is characterized by a high barrier against the final absorption step realized, for instance, by a row of impurity atoms along the dislocation core. In this case, the dislocation would act as a poor sink for SIAs and the annihilation would therefore occur in a reaction limited mode.

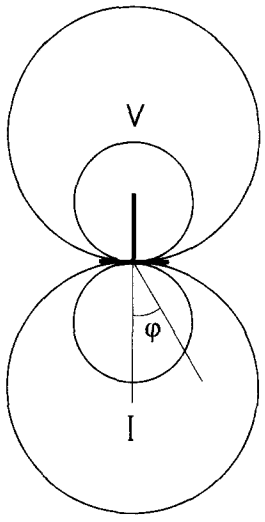


Fig. 7. Equipotential lines for the interaction of a point defect with an edge dislocation. Regions favoured by SIAs and vacancies are indicated by I and V, respectively.

### 3.1. Defect concentrations near dislocations

For distances larger than $r_o$, the elastic dipole approximation may be used to describe the stress/strain induced changes in the equilibrium and saddle point energies of the defects as

$$E^{e,s}(r) = -\mathbf{Q}^{e,s} \cdot \boldsymbol{\sigma}(r), \quad \text{with trace}\,\mathbf{Q}^{e,s} = \Delta V^{e,s}, \quad (1)$$

where $\mathbf{Q}^{e,s}$ is the strain tensor and $\Delta V^{e,s}$ is the relaxation volume of the defect in the equilibrium and saddle point configuration, respectively, and $\boldsymbol{\sigma}(r)$ is the elastic stress tensor field induced by the dislocation [34]. Since $\boldsymbol{\sigma}(-r) = -\boldsymbol{\sigma}(r)$, the angular dependence of the interaction energy is characterized by attractive and repulsive directions with a vanishing directional average (see Fig. 7).

The flux density of defects in such a potential energy mountain is given in compact form by [35]

$$j(r) = -D(r)\exp(-\beta E^e(r))\nabla \exp(+\beta E^e(r))c^e(r), \quad (2)$$

with

$$D(r) = D_\infty \exp(-\beta(E^s(r) - E^e(r)), \quad \beta = 1/kT,$$

where $D(r)$ is the ($r$-dependent) diffusion coefficient, $D_\infty = D(r \to \infty)$ and $c^{e,s}(r)$ are the defect concentrations in the metastable equilibrium and the saddle point positions, respectively. Note that in local equilibrium $\exp(\beta E^e(r))c^e(r) = \exp(\beta E^s(r))c^s(r)$. In the following we need to consider only $c^e(r)$ and we therefore omit the superfix e.

In steady state, the defect flux to a dislocation is determined by defect production and annihilation in the environment. Ignoring mutual recombination and assuming a defect production (displacement) rate $P$ and a sink strength $Zk^2$, we may express continuity under a steady state by

$$\text{div}\, j(r) = P - DcZk^2, \quad (3)$$

where the absorption efficiency or bias factor $Z$ is introduced to later account for differences in the sinks strength for SIAs and vacancies. We note here that the neglect of recombination (which may crudely be accounted for in a reduced effective displacement rate) does not affect the main conclusions.

In general, solutions of Eq. (3) subject to appropriate boundary conditions are complicated because of the complicated angular dependence of $E^{e,s}(r)$. Several simplifying approximation concerning the right hand side of Eq. (3) as well as the quantities $\mathbf{Q}^{e,s}$ and $\sigma(r)$ in Eq. (1) can be made without affecting the general conclusions to be drawn from the results. Since the majority of the defects (SIAs) accumulating in the vicinity of the dislocation are not produced there but come from outside, $P$ at the right hand side of Eq. (3) may be neglected. For establishing the conditions for defect accumulation near a dislocation it is sufficient to consider the initial stage where the second term at the right hand side of Eq. (3) may be neglected too. Both assumptions imply that the extension of the region of efficient interaction, $r \le r_t$, is small compared to the overall diffusional mean free path $\lambda = k^{-1}$, i.e., $r_t \ll k^{-1}$. Under these conditions, we may start from $\text{div}\, j(r) = 0$. In this case, $P - DcZk^2$ enters only via the embedding of the dislocation and its close environment into the effective medium.

On the other hand, the strain tensor $\mathbf{Q}^{e,s}$ may be assumed to be isotropic and the difference between the equilibrium and the saddle point configuration may be

Table 1
Relaxation volumes of self-interstitial atoms, $\Delta V_i$, and vacancies, $\Delta V_v$, in the unit of atomic volume [36]

| | fcc | | | | | bcc | |
|---|---|---|---|---|---|---|---|
| | Al | Ni | Cu | Pt | Au | Fe | Mo |
| $\Delta V_i/\Omega$ | 1.9 | 1.8 | 1.55 | 1.8 | – | 1.1 | 1.1 |
| $\Delta V_v/\Omega$ | −0.05 | −0.2 | −0.25 | −0.2 | −0.15 | −0.05 | −0.1 |

neglected (except for the barrier against the final absorption step in the second case illustrated in Fig. 5b). Assuming further elastic isotropy, the energy of a defect of relaxation volume $\Delta V$ in the strain field of an edge dislocation of Burgers vector $b$ may be written as [34]

$$E(r) = -(A\cos\varphi)/r, \quad \text{with } A = \frac{1}{3\pi}\frac{1+\nu}{1-\nu}\mu\Delta V b, \tag{4}$$

where $r$ is the distance between the defect and the dislocation, $\varphi$ is the angle between the distance vector and the direction of maximum dilation (see Fig. 7), $\nu$ is Poisson's ratio and $\mu$ is the shear modulus of the medium. An estimate on a homologous basis, $A \approx 7kT_m b\Delta V/\Omega$, is obtained by assuming $\nu = 1/3$ and $\mu\Omega \approx 35kT_m$ [6,7] where $\Omega$ is the atomic volume and $T_m$ is the melting temperature. This corresponds to an upper bound estimate for the effective trapping radius given by $r_t = \beta A = 7(T_m/T)(\Delta V/\Omega)b$ ($\approx 20b$ for $T = 0.35T_m$ and $\Delta V = \Omega$).

In the present context, the difference between the values of $\Delta V$ for SIAs and vacancies in metals is important. $\Delta V/\Omega$ is positive for SIAs with values between 1 and 2, and it is negative for vacancies with values between −0.05 and −0.25 (see Table 1). Thus, according to Eq. (4), the interaction is not only opposite (and attractive in opposite directions) but also considerably weaker (by an order of magnitude) for vacancies than for SIAs.

For solving Eq. (3), the boundary conditions must be specified. Close to the dislocation core, thermal equilibrium defines the defect concentrations [37,38]. Since the corresponding values are negligible compared to typical irradiation induced defect concentrations in the temperature range of interest (annealing stage IV), even though their relative local variations may be very large, we may assume $c \to 0$ for $r \to 0$. For large $r$, $c$ must reach a direction independent value to be determined by an appropriate embedding procedure. Under these and the other conditions mentioned above ($r_t \ll k^{-1}$) the complicated general solution [38] for Eq. (3) with $P - Dck^2 = 0$ together with Eqs. (2) and (4) simplifies to [37]

$$c(r) = CF(r), \quad \text{with } F(r) = (2\pi)^{-1}\exp[\beta A(\cos\varphi)/2r]K_0(\beta A/2r), \tag{5a}$$

where $K_0$ is the modified Bessel function of zero order and $C$ is an integration constant to be determined by the embedding procedure. This is done by considering an appropriately weighted partitioning of the defects over the available sinks. Thus, the total defect flux per unit length to one dislocation, defined by the behaviour of Eq. (5a) for $r \to \infty$ as $I = 2\pi rj(r \to \infty) = DC$, must be equal to the production rate, $P$, per overall sink strength, $k^2$, weighted by the ratio of the dislocation bias factor, $Z^d$, to the average bias factor, $Z$. This yields

$$C = Z^d P/DZk^2. \tag{5b}$$

Principally, the solution of the complete Eq. (3) including the right hand side is required to determine the dislocation bias factor $Z^d$. A reasonable approximation is obtained by matching the approximate solution according to Eqs. (5a) and (5b), valid for $r \ll k^{-1}$, at an intermediate distance $R$ satisfying $r_t \ll R \ll k^{-1}$, to the cylindrically symmetric solution of the complete Eq. (3) for vanishing interaction, valid for $r \gg r_t$, with the following result for the dislocation bias factor $Z^d$

$$Z^d = 2\pi/|\ln e^{2\gamma}k\beta A/8|, \tag{6}$$

where $\gamma = 0.5772$ is Euler's constant and $R$ cancels out.

In Fig. 8, the spatial dependence of the defect concentration near a dislocation is illustrated in plots of $F(r)$ vs. $r$ as given by Eq. (5a) for the directions of maximum attraction and repulsion ($\varphi = 0$ and $\varphi = \pi$ for SIAs), respectively. Fig. 8 shows clearly that even on the attractive side the defect concentration decreases monotonically with decreasing distance from the dislocation — opposite to what one could expect intuitively. This decrease occurs in spite of the contraction of the effective cross section for the defect flux with decreasing distance from the disloca-

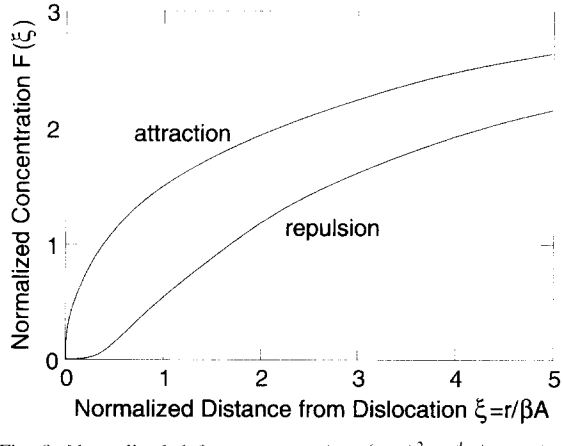


Fig. 8. Normalized defect concentration, $(DZk^2/Z^dP)c = F(\xi)$ vs. normalized distance from the dislocation, $\xi = r/\beta A$, for maximum attraction and repulsion, respectively, according to Eqs. (5a) and (5b).

tion, an (thus invalid) argument for enhanced SIA accumulation used by Kiritani [16].

The reduction of the concentration of each type of point defect everywhere close to the dislocation even on the respective attractive side is, however, not sufficient to rule out enhanced agglomeration of one or the other type of cluster since the nucleation and growth of such clusters is controlled by the *difference* in the absorption of SIAs and vacancies rather than by the absorption of just one of these two types of defects.

### 3.2. Cluster growth near dislocations

The minimum requirement for the accumulation of a certain type of defect in a corresponding type of cluster is that an existing cluster of this type is able to grow. In the framework of the standard rate theory approach, the accumulation of defects in clusters, say of SIAs in SIA clusters, ic, may be described by the increase of the concentration of these defects in clusters as

$$\dot{c}_{ic} = \left( D_i c_i Z_i^{ic} - D_v c_v Z_v^{ic} \right) k_{ic}^2, \tag{7}$$

where $D_i$, $D_v$ are the diffusion coefficients, $c_i$, $c_v$ are the concentrations and $Z_i^{ic}$, $Z_v^{ic}$ are the bias factors for the absorption by clusters of SIAs and vacancies, respectively, and $k_{ic}^2$ is the sink strength of the clusters. An analogous expression holds for vacancies in vacancy clusters. For steady state, the defect flux quantities $D_i c_i$ and $D_v c_v$ may be expressed by the production rates $P_{i,v}$, and sink strengths $Z_{i,v} k^2$ using Eq. (3) (recombination ignored), and their spatial dependencies close to a dislocation may be accounted for by using Eqs. (5a) and (5b), according to

$$D_{i,v} c_{i,v}(r) = \frac{P_{i,v}}{Z_{i,v} k^2} \begin{cases} 1 & \text{globally,} \\ Z_{i,v}^d F_{i,v}(r) & \text{locally,} \end{cases} \tag{8}$$

where $k^2$ is the total sink strength, $Z_{i,v}$ are the average bias factors, $Z_{i,v}^d$ are the dislocation bias factors and $F_{i,v}(r)$ are the functions defined by Eq. (5a) using in the constant A the specific values $\Delta V_{i,v}$ for the relaxation volume of SIAs and vacancies, respectively. Using Eq. (8) with $P_i = P_v = P$ (no 'production bias' [6]) we may write Eq. (7) in the general form

$$\dot{c}_c = \Delta(r) P k_c^2 / k^2, \tag{9}$$

where we have introduced a kinetic factor $\Delta(r)$ for clusters growth as the growth rate of the density of defects in clusters $c$ per unit displacement dose and fractional sink strength, according to

$$\Delta(r) = Z_i^c / Z_i - Z_v^c / Z_v \quad \text{globally} \tag{10a}$$

$$\Delta(r) = \left( Z_i^c Z_i^d / Z_i \right) F_i(r) - \left( Z_v^c Z_v^d / Z_v \right) F_v(r) \quad \text{locally.} \tag{10b}$$

$\Delta(r)$ is defined such that it is positive for the growth of SIA clusters and the shrinkage of vacancy clusters, and negative for the shrinkage of SIA clusters and the growth of vacancy clusters.

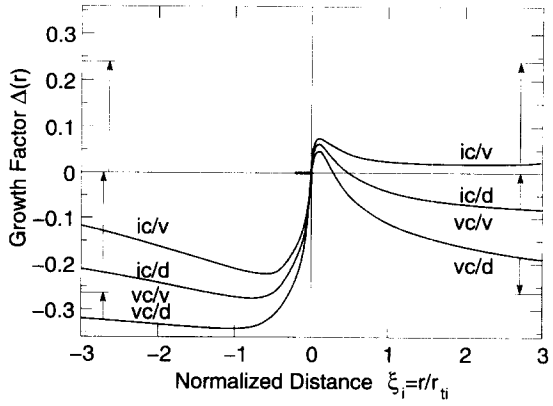


Fig. 9. Kinetic factor for cluster growth, $\Delta(r)$, defined by Eqs. (10a) and (10b) vs. distance from the dislocation, $r$, normalized to the SIA trapping radius $r_{ti} = \beta A_i$ ($\approx 8$ nm) for SIA (ic) and vacancy clusters (vc) in a microstructure dominated by dislocations (d) and voids (v), respectively. $\Delta(r)$ is positive for SIA cluster growth and vacancy cluster shrinkage and negative in the opposite cases. The differences to values of $\Delta(r)$ away from the dislocation are indicated by arrows at the left and right hand sides. The curves for the combinations ic/d and vc/v are identical for the assumptions made.

For the further discussion, we assume that (even small) dislocation loops are characterized by the same bias factors as dislocations, $Z_{i,c}^{ic} = Z_{i,v}^d$ (which are, of course, different for SIAs and vacancies) and that all types of vacancy clusters including cavities and stacking fault tetrahedra are 'neutral', $Z_{i,v}^{vc} = 1$. Under these assumptions we then consider growth (or shrinkage) of SIA (ic) and vacancy (vc) clusters for the two extreme microstructural conditions of dislocation (d) and vacancy cluster (v) dominance. For the corresponding four combinations ic/v, ic/d, vc/v, vc/d, the cluster growth factors $\Delta(r)$ defined by Eqs. (10a) and (10b) are plotted against the distance from the dislocation in Fig. 9. The differences to values far away from the dislocation are indicated at the left and right hand side by arrows. To illustrate the effect of the interaction of vacancies with a dislocation on cluster growth near the dislocation we overestimate the vacancy relaxation volume to be $\Delta V_v = \Delta V_i / 5 = 0.3\Omega$ (see Table 1) such that the effective trapping radius for vacancies reaches 1.6 nm as compared to 8 nm for SIAs at $T = T_m/3$. The dislocation bias factors $Z_{i,v}^d$ have been calculated with use of Eq. (6) for $k^2 = 10^{12}$ m$^{-2}$ and $T = T_m/3$ to $Z_i^d = 1.09$ and $Z_v^d = 0.85$ corresponding to a relative bias factor of $Z_i^d / Z_v^d = 1.28$.

Fig. 9 shows that the SIA cluster growth rate is reduced at the dilatational side of the dislocation ($\xi > 0$) compared to the growth rate far away from the dislocation for a sink structure dominated by (neutral) vacancy clusters (ic/v). When dislocations dominate (ic/d), existing SIA clusters would even shrink ($\Delta(r) < 0$) for not too small reduced

distances $\xi = r/r_{ti} > 0$. Only very close to the dislocation, at $\xi \leq 0.5$, the growth factor $\Delta(r)$ for the case ic/d becomes positive due to vacancy depletion there, and SIA cluster growth would be formally 'enhanced' there since far away from the dislocation $\Delta(r)$ vanishes in this special case. Close to the dislocation, $\Delta(r)$ remains, however, at a low level and the maximum is at $\xi \approx 0.1$ corresponding to distances less than 1 nm where, in fact, SIA depletion rather than accumulation is observed experimentally. The negative values of $\Delta(r)$ for the ic/v and ic/d curves at the compressive side of the dislocation ($\xi < 0$) show that SIA clusters cannot develop there under any microstructural conditions.

From these results we may conclude that the accumulation of SIAs in the form of clusters near dislocations over regions of tens of nm cannot be rationalized in terms of the production, three-dimensional diffusion and agglomeration of single SIAs. This conclusion does not change qualitatively in the case of a production bias, $P_i \neq P_v$, associated with defect cluster production in cascades. Thus, a higher production rate of single SIAs, $P_i > P_v$, would result in an increase of SIA cluster growth. However, this increase is smaller for clusters close to a dislocation than for those that are far away from it. In the opposite case, $P_v > P_i$, SIA cluster growth would be reduced far away as well as close to the dislocation, without changing the relation between both regions qualitatively.

The results for vacancy cluster growth are quite different as shown in Fig. 9. In the case of void dominance (vc/v), vacancy cluster growth may be enhanced even in the dilatational region, but the enhancement is more pronounced in the compressive region and is not affected by the overall sink character (vc/v as well as vc/d). This enhancement occurs over a distance of several $r_{ti}$ corresponding to tens of nm and is due to SIA depletion rather than to the interaction of vacancies with the dislocation which is restricted to a much narrower range (less than 1.6 nm). Accordingly, the accumulation of stacking fault tetrahedra in a wide region (about 20 to 30 nm) adjacent to a dislocation in electron irradiated silver as shown in Fig. 1 may be explained by substantial SIA depletion in that region.

Finally, we return to the second case illustrated in Fig. 6b (dislocation as a poor sink, reaction limited SIA annihilation). In this case, the SIA concentration close to the dislocation increases with time until it has established a kind of Cottrell cloud [25] with a quasi-equilibrium distribution

$$c_i(\boldsymbol{r}) \approx c_\infty \exp(-\beta E^e(\boldsymbol{r})). \tag{11}$$

According to Eq. (11), the SIA concentration is strongly enhanced in a region on the attractive side of the dislocation where $\beta E^e(r) < -1$, occurring for $r < 20b$ at temperatures around $T_m/3$. This enhancement is even accentuated in the SIA clustering rate which depends at least quadratically upon the SIA concentration. SIA clustering will therefore be particularly high in the immediate vicinity of the dislocation core. This behaviour is opposite to that in the diffusion limited case described by Eqs. (5a) and (5b). SIA precipitation at the core of the original dislocation will, however, lead to a reconstruction of a new clean dislocation suppressing further SIA clustering as discussed above for the first case. We emphasize here that blocking of dislocations by impurities is anyway very unlikely in well annealed pure metals where decoration of dislocations with loops has been found to be most pronounced.

So far, we have assumed that the diffusion of the SIAs is three-dimensional and concluded that, in this case, no enhanced SIA clustering would occur near dislocations. In the present context, we should also consider the possibility of SIAs produced in the crowdion configuration which would be constrained to one dimension and thus could be trapped by a dislocation without getting absorbed by it. There is, however, general consensus that in the strong distortion field of a dislocation crowdions, even if they were metastable in the undistorted lattice, would readily convert to the three-dimensionally migrating dumb-bell configuration which would annihilate at the dislocation. In the following section, we shall, however, consider the possibility of a one-dimensional migration of defects produced in the perfect loop configuration (coupled crowdions [29]).

We may summarize this section by stating that the observed decoration of dislocations with SIA loops is most likely not due to a preferential clustering of single SIAs in the neighbourhood of such dislocations.

## 4. Accumulation of glissile loops near dislocations

It is now well established that in displacement cascades a substantial fraction of SIAs are produced in the form of clusters [27–30] and that some of these clusters are glissile [29]. Such a loop may perform a thermally activated random glide motion until it gets trapped in the strain field of another defect cluster or a dislocation [6,7].

There are two important aspects in the kinetics of one-dimensionally migrating defects in comparison to the kinetics of three-dimensionally migrating defects: (1) the range of free migration and (2) the frustrated absorption once the defect is trapped in the strain field of another defect. The crucial quantity characterizing the range of a one-dimensionally migrating defect is its mean free path. For a defect of configuration $i$ migrating one-dimensionally in a crystal containing a number density $c_j$ of defects of configuration $j$ with effective interaction cross section $\sigma_{ij} = \pi r_{ij}^2$ and a line density $\rho$ of dislocations with effective interaction diameter $d_i$ the reciprocal mean free path $\kappa_i = \lambda_i^{-1}$ is given by [6,7]

$$\kappa_i = \lambda_i^{-1} = \sum_j \sigma_{ij} c_j + d_i \hat{\rho}, \tag{12}$$

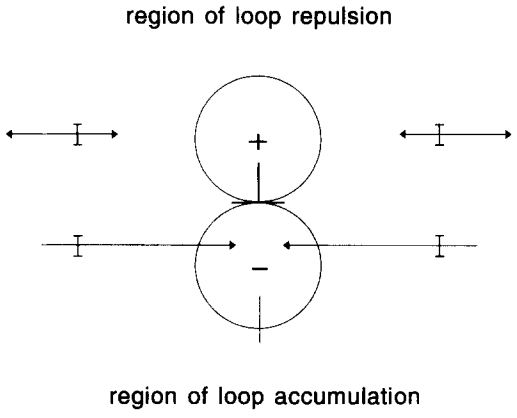


Fig. 10. Sketch of regions of strong attractive and repulsive elastic interaction between an interstitial type dislocation loop and a straight edge dislocation. Loop accumulation will occur in the region of strong attractive interaction.

where $\hat{\rho} = \pi\rho/4$ is the dislocation line length per unit volume projected on a plane perpendicular to the migration direction. $\sigma_{ij}$ and $d_i$ are determined by the mutual elastic defect interaction.

The most striking feature resulting from Eq. (12) is that for low and moderate defect densities, $C_i$ and $\rho$; the ranges of small glissile loops are of the order of several μm and are thus significantly larger than for three-dimensionally migrating point defects. Consequently, the microstructural evolution occurs, particularly at low doses and in well annealed pure metals in a very heterogeneous fashion characterized by a large-scale segregation of SIA-type and vacancy type defects. Under such conditions, a grown-in dislocation would have a large drainage area for accumulating glissile loops in its neighbourhood.

As for a single SIA, the elastic dipole approximation for the interaction of a small loop with the stress field of another defect such as a dislocation is given by Eq. (1) (see Fig. 10). For a loop, the strain tensor may be written as

$$Q_{kl} = A_k b_l, \quad \text{with } \boldsymbol{A}\cdot\boldsymbol{b} = A_k b_k = n_i\Omega, \tag{13}$$

where $\boldsymbol{A}$ is the area vector of the loop, $\boldsymbol{b}$ is its Burgers vector (BV) and $n_i$ is the number of SIAs in the loop. A small glissile loop is assumed to perform a virtually free thermally activated one-dimensional random walk as long as the interaction with other defects is below $kT$ (region 1 in Fig. 12). The motion of a loop will be significantly affected by the interaction where this is larger than $kT$ (region 2–5 in Fig. 12). Using $\mu\Omega \approx 35kT_m$ [6,7] in estimating the magnitude of the interaction energy we write

$$|E| \le 0.35\mu\Omega n_i/r \approx 12bn_i kT_m/r, \tag{14a}$$

$$|E| \ge kT \quad \text{for } r \le 12bn_i T_m/T. \tag{14b}$$

The angular dependence of the interaction energy is characterized by attractive and repulsive directions as sketched in Fig. 10. Glissile loops will be trapped at the attractive side. It should be noted that the upper bound estimates for the interaction energy and the range where its magnitude is larger than $kT$ as given by Eqs. (14a) and (14b) are meant for the most strongly interacting dislocation/loop configuration (both mainly of edge type, parallel BVs) and are thus substantially higher than the estimates for the 'average interaction' given in Refs. [6,7]. According to Eq. (14b) a maximum range as high as 90 nm is estimated for $b = 0.25$ nm, $n_i = 10$ and $T = T_m/3$.

Except for a direct encounter of a glissile loop with a dislocation, the loop will generally be trapped in a metastable state. Absorption of such a loop by the dislocation requires a change in the direction of motion of the loop either by a thermally activated BV change or by conservative ('self') climb via core diffusion, or a mutual approach of the loop and the dislocation by a joint motion in the case of non-parallel BVs (see Fig. 11). In the latter case, the loop would be readily absorbed. In the former case the real fate of a trapped loop depends, via the interaction energy, on its distance from the dislocation (see Fig. 12). In the outer part of the trapping region (region 2), thermally activated detrapping will dominate but the interaction with other loops or even loop clustering in this region may impede detrapping. Somewhat closer to the dislocation (region 3), thermally activated BV changes and/or conservative climb will dominate. In approaching the dislocation further, the barrier against BV changes or climb may disappear and the motion may become unstable (region 4). When the loop comes very close (i.e., within a few $b$) to the dislocation (innermost region 5) it may disintegrate in a kind of melting process and get incorporated into the dislocation [24]. Because of their relatively high mobility, isolated small loops will not form strong obstacles for glissile dislocations but will be sucked in by such dislocations [26].

The density of loops built up in the neighbourhood of a dislocation will depend on the loop arrival rate determined

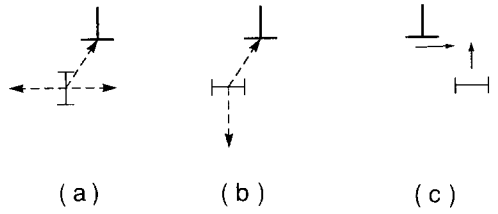


Fig. 11. Possible configurations for the trapping and absorption of a glissile loop by a dislocation segment, (a) metastable trapping state for parallel Burgers vectors, (b) metastable trapping state at a sessile dislocation segment for nonparallel Burgers vectors, (c) absorption of a loop by a joint motion with a glissile dislocation segment. In cases (a) and (b), absorption requires Burgers vector change or climb of the loop.

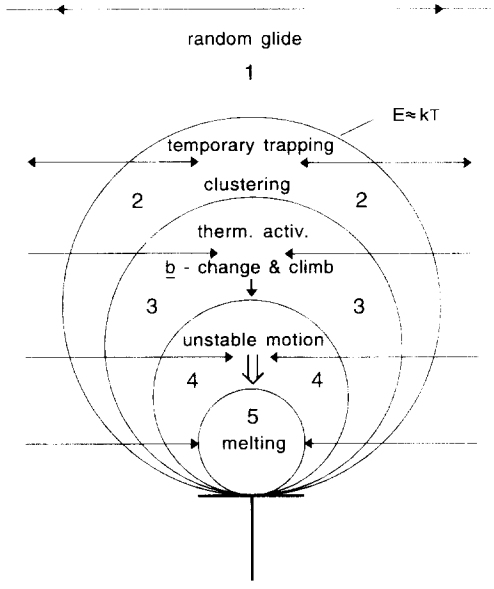


Fig. 12. Sketch of characteristic regions in the interaction of a glissile interstitial loop with an edge dislocation. In region 1, $|E| \leq kT$, the loop performs a one-dimensional random walk motion. In regions 2–5, $|E| \geq kT$, the motion of the loop is significantly affected by the interaction with the dislocation. In region 2, thermally activated detrapping dominates over changes in the direction of motion of the loop but the interaction with other loops may impede detrapping. In region 3, thermally activated BV changes and/or conservative climb dominate. In region 4, the loop motion becomes unstable and, in region 5, the loop disintegrates and gets incorporated into the dislocation.

by the cascade induced glissile loop production rate and the loop trap (dislocation) density. For low loop arrival rates (low loop production rate/high dislocation density) loop interaction and clustering is negligible. In this case, the outer boundary of the region where BV changes and climb becomes dominant (region 3) defines the loop absorption range of the dislocation. For high loop arrival rates (high loop production rate/low dislocation density), loop interaction and clustering will reduce the detrapping rate as well as the rate of BV change and climb. In addition, loops may become sessile by faulting. These processes will lead to an accumulation of loops in the corresponding regions (region 2 and 3). Thus, for the limiting case of very high loop arrival rates, the initial extension of the region of decoration is given by the boundary of the trapping region (90 nm in the above example). Virtually no loop accumulation will occur in the inner regions of rapid unstable approach (4 and 5) where the loop density is expected to remain very low. Accordingly, the extension of these regions defines the 'stand-off distance' [24] between the loop ensemble and the dislocation.

For a quantitative estimate of the loop behaviour in the most important regions of possible loop accumulation 2 and 3, thermally activated BV changes and conservative climb must be considered in some detail. For the average time between two BV changes we may assume an Arrhenius behaviour

$$\tau_b = \tau_0 \exp(\beta E_b), \tag{15}$$

where the pre-exponential term $\tau_0$ is estimated to be of the order of $10^{-13}$ s. Unfortunately, not much is known about the activation energy $E_b$. In MD studies of cascade defects in Cu, the change in the BV of a cluster consisting of four SIAs ('coupled crowdions') has been observed [29]. From the life time of a given configuration a relatively low value of 0.4 eV has been estimated for the barrier against this transformation. $E_b$ certainly increases with increasing loop size and would be proportional to $n_i^{1/2}$ if the BV change were controlled by the sweeping of a partial dislocation across the loop area.

The drift velocity of a loop climbing in a force field is given by

$$\boldsymbol{v}(\boldsymbol{r}) = -\beta \mathbf{D}_l \nabla E(\boldsymbol{r}), \tag{16}$$

where $\mathbf{D}_l$ is the (two-dimensional) diffusion tensor of the loop. Below 0.5 $T_m$, the fastest climb mechanism is conservative 'self-climb' by dislocation core diffusion the activation energy of which may be expected to be comparable with those for self-diffusion along dislocations and grain boundaries [7] which are around $9kT_m$. This conservative loop climb is characterized by a loop diffusion coefficient, $D_l$, which is proportional to the dislocation core diffusion coefficient $D_{dc}$ and decreases with increasing size $n_i$ as $D_l \approx D_{dc}/n_i^{3/2}$. Integrating Eq. (16) for $E(r) \propto 1/r$ we may estimate the time required for a loop to reach the dislocation as

$$\tau_c \approx r^2/[3\beta E(r) D_l]. \tag{17}$$

The quantitative evaluation of these processes remains uncertain, particularly for BV changes because of the uncertainty concerning their activation energies. We may, however, deduce lower bound estimates for the activation energies of both processes simply on the basis of the experimental fact that decoration of dislocations by loops occurs and in our view this must be due to the capture of glissile loops by such dislocations. Because of the low values of the activation energy for thermally activated glide, the glissile loop concentration between the existing dislocations (similar as the single SIA concentration) will reach quasi-steady state very soon after the beginning of irradiation. In this situation, the rate of absorption of loops by sinks equals their production rate, $P_l$. Assuming for the moment that the glissile loops are really absorbed by dislocations their flux per unit length may be expressed by their density per unit length within the trapping region, $N_l$, over the average time required by them to reach the dislocations by BV change and climb (without being detrapped before) $\tau_{b,c}$. Assuming furthermore that the dislo-

cations of density $\rho$ form the dominant sinks for glissile loops we may write the balance equation as

$$P_l = \rho N_l / \tau_{b,c}. \quad (18)$$

Using this equation, $N_l$ could be estimated if the other quantities were known. Assuming, for instance, $P_l\Omega = 10^{-2}P_d\Omega = 10^{-8}$/s, where $P_d\Omega$ is the NRT displacement rate, $\rho = 10^{12}/m^2$ and $\tau_b$ values estimated on the basis of MD [29] and Eq. (15) for four coupled crowdions at $0.4T_m$, we find a negligibly small value of about 5/m meaning that such clusters would be virtually instantaneously absorbed by dislocations, like single crowdions, and thus would not contribute to decoration. In fact, loop interaction and immobilization by clustering would require a sufficiently large loop density per unit dislocation length, say at least 1/100 nm. Leaving the other numbers unchanged we obtain with this condition lower bound estimates for the activation energies for BV change and climb which would allow loop immobilization by agglomeration. Using Eqs. (15) and (17) we find $E_b \geq 9kT_m$ for both BV change and climb. The relatively large lower bound value for $E_b$ compared with the value for four coupled crowdions means that the glissile loops contributing to decoration must be substantially larger than this configuration, perhaps up to $n_i \approx 20$. Our above assumed activation energy of $9kT_m$ for climb is consistent with decoration up to about $0.4T_m$.

Under these conditions, loop absorption by a dislocation would be sufficiently reduced to allow mutual blocking by accumulation in regions 2 and 3. Loop clustering may be described similarly as for single defects. The formation rate of closely bound loop pairs will be enhanced in region 2 at least by a factor of $e^2 \approx 7.4$ according to a second order chemical reaction. Thus the primary extension of the region of decoration may be of the order of 100 nm as estimated by Eq. (14b). We do not discuss details here but confine ourselves to a qualitative description of the decoration process. The conditions for the occurrence of loop accumulation near dislocations will be discussed in more detail elsewhere [39].

In Fig. 13, the characteristic phases of the decoration process are sketched schematically. In the first phase, loop trapping in the region of strong attractive interaction occurs resulting in loop accumulation in spite of partial detrapping and absorption; loop clustering and growth (coarsening) are still negligible; quasi-equilibrium concentration ('Cottrell cloud') and quasi-steady state concentrations of loops are established in regions 2 and 3 of Fig. 11, respectively. The second phase is characterized by loop agglomeration and growth under continued loop trapping; a repulsive force against further loop trapping gradually builds up. In the third phase, loop trapping ceases and the SIA content in the primary trapping region saturates since the attractive stress field of the leading dislocation is now fully compensated by the existing loops. Concerning the stress field, the whole dislocation/loop configuration is equivalent to a dislocation shifted by the extension of the primary region of loop trapping. Loop trapping occurs now only ahead of the existing structure where the elastic interaction remains attractive. Accordingly, the structure grows by further loop trapping in the direction where the interaction is strongest, i.e., away from the leading dislocation, and begins to form a dislocation wall there. In a possible late fourth phase the supply of glissile loops may exhaust due to the overall build-up of the microstructure. In such a phase, loop coarsening may result in a shrinkage or even disappearance of the pronounced structures occurring in the third phase.

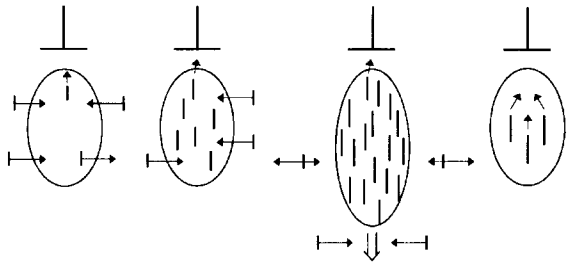

Fig. 13. Sketch of characteristic phases in the decoration of dislocations with loops: (1) loop accumulation by trapping in region of strong attractive interaction; loop clustering negligible; (2) loop clustering and growth (coarsening) under continued trapping; building up of repulsive counter force field; (3) saturation of SIA content in the primary region of loop accumulation; growth of the structure by loop trapping away from the dislocation resulting in wall formation; (4) exhaustion of loop supply due to the overall build-up of the microstructure; coarsening, shrinkage and disappearance of the loop structure.

This scenario is able to explain the observed features of the decoration of dislocations by small dislocation loops. The specific conditions for the occurrence of the processes will be discussed elsewhere [39].

## 5. Conclusions

In many microstructural studies of neutron irradiated metals segregation of small dislocation loops of SIA type in the vicinity of grown-in dislocations in the form of a 'Cottrell-like' atmosphere, or in 'rafts' of loops and 'walls' of loops and dislocation segments has been observed. In the present paper, possible mechanisms for this phenomenon associated with cascade damage conditions have been considered. The main conclusions may be summarized as follows.

(1) The phenomenon cannot be rationalized in terms of strain enhanced agglomeration of single three-dimensionally migrating SIAs since the strain field of a dislocation induces a depletion not only in the compressive but also in the dilatational region resulting in reduced rather than enhanced agglomeration of SIAs. SIA depletion, particularly at the compressive side, may, however, induce en-

hanced vacancy agglomeration as has been occasionally observed after electron irradiation.

(2) The present analysis suggests that the trapping and accumulation of SIAs near dislocations would require a restriction of the dimension of the SIA migration which is most efficient for the case of a strictly one-dimensional motion. Any transversal component in the motion or a discrete change in the migration direction must be relatively small or rare, respectively, to ensure efficient SIA accumulation. It seems highly unlikely that a possibly metastable one-dimensionally migrating crowdion could fulfill this requirement since this defect configuration would certainly be unstable in the strong distortion field of a dislocation. Coupled crowdions in the form of glissile perfect SIA loops, on the other hand, could easily fulfil this requirement. We, therefore, consider the decoration phenomenon to be due to the glide and trapping of glissile SIA loops directly produced in cascades.

(3) Small loops trapped in the strain field of a dislocation may be detrapped by thermal activation. Before this occurs they may approach the dislocation by thermally activated changes in the Burgers vector and/or by conservative climb. Thus, decoration of dislocations with loops requires that a single trapped loop is immobilized by other loops before it is detrapped from or absorbed by the dislocation. This requirement makes the dislocation decoration phenomenon dependent upon the dislocation density, the loop production rate, the rate of Burgers vector change, the climb velocity and temperature. More detailed modeling is needed to establish these dependencies quantitatively.

## References

[1] A.D. Brailsford, R. Bullough, Philos. Trans. R. Soc. (London) 302 (1981) 87.
[2] L.K. Mansur, in: Kinetics of Nonhomogeneous Processes, ed. G.R. Freeman (Wiley–Interscience, New York, 1989).
[3] J.O. Stiegler, E.E. Bloom, Radiat. Eff. 8 (1971) 33.
[4] B.N. Singh, T. Leffers, W.V. Green, S.L. Green, J. Nucl. Mater. 105 (1982) 1.
[5] A. Horsewell, B.N. Singh, ASTM-STP 955 (1988) 220.
[6] H. Trinkaus, B.N. Singh, A.J.E. Foreman, J. Nucl. Mater. 206 (1993) 200.
[7] H. Trinkaus, B.N. Singh, C.H. Woo, J. Nucl. Mater. 212–215 (1994) 18.
[8] B.N. Singh, S.J. Zinkle, J. Nucl. Mater. 206 (1993) 212.
[9] J.L. Brimhall, B. Mastel, Radiat. Eff. 3 (1970) 203.
[10] V.K. Sikka, J. Moteff, J. Nucl. Mater. 54 (1974) 325.
[11] J. Bentley, B.L. Eyre, M.H. Loretto, US-ERDA Conference 751006, Gatlinburg, 1975, p. 925.
[12] J.H. Evans, J. Nucl. Mater. 88 (1980) 31.
[13] K. Yamakawa, Y. Shimomura, J. Nucl. Mater. 155–157 (1988) 1211.
[14] B.N. Singh, J.H. Evans, A. Horsewell, P. Toft, D.J. Edwards, J. Nucl. Mater. 223 (1995) 95.
[15] B.N. Singh, J.H. Evans, to be published.
[16] M. Kiritani, Mater. Sci. Forum 15–18 (1987) 1023.
[17] S. Kojima, T. Yoshiie, M. Kiritani, J. Nucl. Mater. 155–157 (1988) 1249.
[18] Y. Satoh, I. Ishida, T. Yoshiie, M. Kiritani, J. Nucl. Mater. 155–157 (1988) 443.
[19] M. Kiritani, private communication.
[20] B.N. Singh, A. Horsewell, P. Toft, D.J. Edwards, J. Nucl. Mater. 224 (1995) 131.
[21] B.C. Larsen, F.W. Young, 'Radiation induced voids in metals, in: Proc. Albany Conf., eds. J.W. Corbett and I.C. Ianniello, USAEC Symposium Services 26, CONF-710601, 1971, p. 672.
[22] B.N. Singh, T. Leffers, A. Horsewell, Philos. Mag. A53 (1986) 233.
[23] C.A. English, B.L. Eyre, J.W. Muncie, Philos. Mag. A56 (1987) 453.
[24] B.N. Singh, A.J.E. Foreman, H. Trinkaus, this issue p. 103.
[25] A.H. Cottrell, Dislocations and Plastic Flow in Crystals (Clarendon, Oxford, 1953).
[26] M.J. Makin, Philos. Mag. 10 (1964) 695.
[27] T. Diaz de la Rubia, M.W. Guinan, J. Nucl. Mater. 174 (1990) 151.
[28] T. Diaz de la Rubia, M.W. Guinan, Phys. Rev. Lett. 66 (1991) 2766.
[29] A.J.E. Foreman, C.A. English, W.J. Phythian, Philos. Mag. A 66 (1992) 655.
[30] A.J.E. Foreman, C.A. English, W.J. Phythian, Philos. Mag. A66 (1992) 671.
[31] M. Suehiro, N. Yoshida, M. Kiritani, Proc. Yamada Conf. V, Point Defects and Defect Interactions in Metals, Univ. Tokio Press, 1982.
[32] W. Sigle, M.L. Jenkins, J.L. Hutchison, Philos. Mag. Lett. 57 (1988) 267.
[33] S.L. King, M.L. Jenkins, M.A. Kirk, C.A. English, J. Nucl. Mater. 205 (1993) 467.
[34] F. Kroupa, in: Theory of Crystal Defects, ed. Gruber (Academic Press, New York, 1966).
[35] P.H. Dederichs, K. Schroeder, Phys. Rev. B17 (1978) 2524.
[36] P. Ehrhart, K.H. Robrock, H.R. Schober, in: Physics of Radiation Effects in Crystals, eds. R.A. Johnson and A.N. Orlov (Elsevier, Amsterdam, 1986).
[37] F.S. Ham, J. Appl. Phys. 30 (1959) 915.
[38] I.G. Margvelashvili, Z.K. Saralidze, Sov. Phys. Solid State 15 (1974) 1774.
[39] H. Trinkaus, B.N. Singh, A.J.E. Foreman, in: Proc. Workshop on Defect Production, Acumulation and Materials Performance in Irradiation Environment, Davos, Switzerland, Oct. 1996, J. Nucl. Mater. 251 (1997) in press.